PREPARATION AND CHARACTERIZATION OF NEW IMINE- FUNCTIONAL GROUP FOR FAST REMOVAL OF Cr (III) IN SOME SUPPLEMENTS FROM SHRIMP SHELL

H. Y. Sharef * **N. A. Fakher ***
Lecturer **Professor**
***Department of chemistry, college of education, Salahaddin university-Erbil, Iraq**
huda.sharef@su.edu.krd **nabil.fakhre@su.edu.krd**

ABSTRACT

A new imine-Schiff base adsorbent is prepared from extracted chitosan to make taking away exoskeletons of crustacean shrimp shells low-cost and environmentally friendly with the fast and high ability to remove Cr (III) from aqueous solution. The resulting composites were verified by different techniques FTIR, H-NMR, FESEM, EDX, XRD. On applying the adsorption kinetic model, the pseudo 2^{nd} order model was best characterised, using adsorption equilibrium data; the Langmuir model provided a superior description. Further, the negative value of ΔG shows a spontaneous process in nature. Finally, the prepared adsorbent has been applied to a real sample of bodybuilder supplements.

Keywords: extracted chitosan, imine-schiff base, removal of Cr (III).

تحضير و دراسة خصائص ايمين الجديد المستخلص من قشور الروبيان لازالة السريعه لأيون الكروم الثلاثي قي بعض المكملات الغذائيه

هدى يوسف شريف نبيل عادل فخري
مدرس أستاذ
قسم الكيمياء – كليه التربية – جامعه صلاح الدين– أربيل – العراق

المستخلص

تم تحضير مادة مازه جديدة من نوع قاعدة شيف من الكيتوسان المستخلص من الهياكل الخارجية من قشور الروبيان ذات تكلفه منخفضه وصديقة للبيئه وذات قدرة عاليه على ازالة الكروم الثلاثي من المحلول المائي . وتم تشخيص المركب الناتج باستخدام تقنيات FTIR, H-NMR, FESEM, EDX, XRD. وتبين ان التفاعل من المرتبه الثانيه الكاذبه وينطبق عليه أنموذج لانكماير, وان قيمه طاقه كبس الحره كانت سلبية دلاله على تلقائية عمليه الامتزازي . وتم تطبيق الطريقه على عينات حقيقيه لبعض المكملات الغذائية .

الكلمات المفتاحية: استخلاص الكيتوسان، ايمين– قاعدة شيف، امتزاز عنصر الكروم الثلاثي , دراسه السلوك الحركي (كاينتيك) والتوازن الامتزازي (ايزوثيرم).

Received:29/3/2022, Accepted:5/6/2022

INTRODUCTION

The most severe environmental problem faced by the world today is heavy metal pollution. Heavy metals are among the most well-recognized chemicals that are hazardous to human health (23). Heavy metal ions in the environment can accumulate in living organisms and get magnified by them (17). The toxicity of foods increases as the quantity of toxins increase (6, 8). The metal finishing uses of chromium include electroplating, textile industries, leather tanning, and magnetic tapes. Chromium may be released into the environment via industrial wastewater discharge. Chromium (VI) molecules are poisons, whereas chromium (III) is vital to human health (27). The techniques for eliminating heavy metal ions from wastewater using traditional methods include chemical precipitation, membrane filtration, ion exchange, activated carbon adsorption, and electrolysis (29). The removal of wastewater, groundwater, and industrial effluents is a competition for adsorption technologies, The use of biological materials, natural substance or biomass as a sorbent in the pollutant removal called biosorption. Biomass has been utilized to adsorb pollution from a variety of sources, including bacteria, yeast, algae, fungi, and plants (21). The most important aspect of the biosorption technique is to choose an effective biosorbent with a large surface area, low price, and high adsorption capacity. Chitosan, for example, is a bio-adsorbent. Cuticles of various crustaceans, mostly crabs, shrimps, and insect exoskeletons, are the main source of raw materials for chitin extraction (16). Chitosan (CS) is a biocompatible, anticoagulant, and nontoxic substance formed from chitin via deacetylation in an alkaline environment (28). CS and its derivatives have many uses in biotechnology, healthcare, culinary additives, and cosmetics. It's a natural polysaccharide with many $–NH_2$ and –OH groups that may act as chelation sites to adsorb heavy metal ions in wastewater treatment (22). Chitosan is soluble in dilute acids. The solubilization occurs by the protonation of the $–NH_2$ function on the C-2 position of the Dglucos amine repeat unit, where the polysaccharide is converted to a polyelectrolyte in acidic media. In acetic acid, chitosan reacts with aromatic aldehydes to create Schiff bases (16). Schiff bases, including an imine group (–RC=N–), are often synthesized by primary amine condensation with an active carbonyl (11). The purpose of this study is to develop a newly modified sorbent by extracting chitosan from shrimp shells and then reacting it with 4-floro Benzaldehyde to create a highly active imine for the rapid removal process of Cr (III) ion from aqueous solution using small quantities. The contact duration time, starting metal concentration, pH, imine-Schiff base dose, and temperature were all utilized as adsorption conditions in this research. Furthermore, the sorbent was studied using a variety of techniques, including FTIR, FESEM, EDX, XRD, and H-NMR. We investigated the maximal adsorption capacity, selective adsorption kinetics, thermodynamics, and reuse. Then, we used serum of athletes and some supplements they took to examine the efficiency of the new adsorbent.

MATERIALS AND METHODS

Reagents: Chitosan (CS) (with DDA 69% from IR chart), 4-florobenzaldehyde, Methanol, NaOH, HCl, CH_3COOH, $Cr_2(SO_4)_3.15H_2O$ These chemicals were used us supplied (B.D.H), (Merk), (Sigma -AL) (Scharlau). All solvents were of analytical reagent grade (AR) and had the highest purity available.

Chitosan extraction from shrimp shell

CS was extracted from shrimp shells (obtained from a local market) that used a conventional technique that included demineralization, deproteination, and deacetylation. The shrimp shells were cleaned, dried, and crushed. Then soaked in boiling NaOH 4 % (w/v) to dissolve protein and sugar. The demineralization of the shell was carried out with 1% HCl for 24h. For the last step, 50% NaOH adding and boiling for 2h at 100°C. Before being dried in a vacuum oven set to 60 degrees Celsius, the product was neutralized in running tap water and washed with distilled water, this procedure reported by Puvvada, et. al. (20).

Chitosan-Schiff base preparation (imine)

The methods documented in the literature were used to produce the CS-Schiff base by Vadivel, et.al. (25). It was synthesized through a condensation process. About 1g of CS

powder was dissolved in 25ml ethanol with three drops of acetic acid and vigorously shaken to produce an emulsion of chitosan. Additionally, 0.87g of 4-florobenzaldehyde was dissolved in 25mL ethanol and added to the CS emulsions. Both solutions were combined and agitated for 30 minutes before the contents were heated for 12 hours in a 60 °C underwater bath. The yellow product was filtered and dried after being rinsed with ethanol(3-((4-fluorobenzylidene)amino)-6-(hydroxymethyl)-2-methoxy-5-methyl tetrahydro-2H-pyran-4-ol).

Characterization of imine

The synthesized imine was characterized in a way that covers a large area. Fourier transfer infrared spectra were carried out (SHIMADZU IR affinity –I FTIR spectrophotometer), the morphologies of particles were observed using SEM coupled with EDX (TESCAN MIRA3 FEG-SEM, Australia) and TEM (FEI TECNAI G2F20 transmission electron microscope). XRD patterns were recorded with an X-ray diffractometer using a Cu Kα spectral line at 45KV and 40 mA, and a 2θ between the ranges of 5 to 80. Finally, 1H-NMR (broker AVANCENEO (400MHZ) spectrometer).

Adsorption procedure

The batch was conducted to investigate the impact of dose using various amounts of sorbent (10, 15.20, 25 and 30 of imine), pH (from 3 to 11), chromium concentration range (30-80mg/L), contact duration (0-24h), and temperature (5-45°C) The new adsorbent (0.02g) was added to a 10mL Cr (III) aqueous solution, which then shaken at room temperature. An FAAS was used to evaluate the residual concentration of Cr ion after adsorption, and the absorbance was measured at 357.9nm with a spectral bandwidth of 0.5 nm. The adsorption capacity utilizing the following equation:

$$qe = (Ce-qe)\ V/m$$

The ions have an equilibrium capacity of adsorption, which is described by the constant concentration ratio of adsorbent Ci (mg L-1) and the initial concentration of ions. Additionally, the initial and final concentrations of metal ions are used to indicate the ion concentrations at the start and the equilibrium of a reaction. The volume of the ion solution is defined by the measurement of volume in liter, and the mass of the polymer is defined by the number m (g). To determine the adsorbent's selectivity, the result of the data adsorption experiments was analyzed. The distribution coefficient was determined as follows:

$$Kd = \frac{Cp}{Ce} \qquad Kd = \frac{Cp}{Ce}$$

The distribution coefficient, Kd (mg/L), is equivalent to the concentration of adsorbed metal ions, Cp (mg. L^{-1}). Equilibrium binding data may be used to calculate the selectivity coefficient for the binding of a Cr (III) ion in the presence of competing species (22).

$$K = \frac{Kd(Cr(III))}{Kd(M)} \qquad K = \frac{Kd(Cr(III))}{Kd(M)}$$

K denotes the selectivity coefficient, and metal ion denotes competing metals. When there are additional metals in the solution, they will attract each other. K indicates Cr (III) ion adsorption selectivity. The higher the K, the better the Cr (III) ion's capacity to choose. The Freundlich, Langmuir, and Temkin. Models have been used to estimate the adsorption data for the mechanism of the adsorption process (2).

The Langmuir equation may have been expressed linearly as follows:

$$\frac{Ce}{qe} = \frac{1}{qmax\ Kl} + \frac{Ce}{qm}\frac{Ce}{qe} = \frac{1}{qmax\ Kl} + \frac{Ce}{qm}$$

Where Ce is an adsorbate concentration in balances (mg. g^{-1}), K is the adsorption-related Langmuir constant (mg. g^{-1}), which may be related to changes in the reasonably normal porosity of the adsorbent that would lead to higher adsorption ability for a bigger surface area and porous volume. In describing the basic characteristics of the Langmuir isotherm,

$$Rl = \frac{1}{1+KLC^{\circ}}Rl = \frac{1}{1+KLC^{\circ}}$$

The separation factor RL is a dimensionless constant. The initial concentration of adsorbate (mg. g^{-1}) is where KL (mg. g^{-1}) constant. When unfavourable RL > 1, linear, when RL = 1, favourable when 0 < RL >1, and irreversible when RL = 0.

While the Freundlich isotherm does have following linear form:

$$\log qe = \log Kf + \frac{1}{n}\log ce$$

$$\log qe = \log Kf + \frac{1}{n}\log ce$$

Where Kf represents the adsorption capacity (L/mg) and 1/n signifies the adsorption intensity; it also reflects the energy distribution and adsorbate site heterogeneity of the adsorbate site. The linear forms of the Timken isotherm may be expressed by the following equation: qe = KT + 2.303 bT log Ce

The Temkin constant (bT) is related to the heat of sorption (Jmol-1) and the Temkin isotherm constant (KT) (L. g-1). The adsorption behaviour during biosorption was investigated using a pseudo1st kinetic model and a pseudo 2nd order kinetic model in this research Pseudo 1st order kinetic model:

$$\log(qe - qt) = \log qe - \frac{K1t}{2.303}$$

pseudo 2nd order kinetic model

$$\frac{t}{qt} = \frac{t}{qe} + \frac{1}{K2qe^2} \qquad \frac{t}{qt} = \frac{t}{qe} + \frac{1}{K2qe^2}$$

Where k1 is the pseudo1st order rate constant (min^{-1}) and k2 is the pseudo 2nd order rate constant (g mg^{-1} min^{-1}). Real sample preparation The efficiency of the Schiff base was evaluated with a determination of Cr (III) ions in some supplicates. The study took a sample from the two types of nutritional supplement tablets that bodybuilders take. The heavy metal content was digested using 1:3 $HClO_3$ and HNO_3. sample was transferred into a tube and 0.02 g of adsorbent was placed, then shaken using thermostat water bath shaker at an optimum condition that was optimized previously. The supplement was applied on imine by batch adsorption and recovery tests and FAAS was used to calculate the heavy metal ions ratio. Then, 25 ml of deionized water (DW) was added to dilute the sample. 10 ml of diluted.

RESULTS AND DISCUSSION

Characterization - FTIR

FTIR spectra are shown in Figure (1). The OH and NH_2 groups' stretch is attributed to the wide peak at 3570-3330 cm^{-1}, whereas the stretching vibration of the (CH) group of the CS backbone is assigned to the peak at 2885cm-1. Other peaks associated with the amide group include those at 1083 cm^{-1}, 1150 cm^{-1}, and 1028cm^{-1} (stretching vibration C-N bond), 1383cm^{-1} (stretching vibration C-O bond), and the sorption peak at 1659cm^{-1} (19,15). The high absorbance band at 1649cm^{-1} for chitosan Schiff base is due to the C=N vibration typical of imine produced among the amino group of chitosan and the carbonyl group of aldehydes Because the free aldehyde group is condensed with a primary amine in the basic of the chitosan monomer, which results in the formation of Schiff -base, these results agree with the finding of Shahraki, et.al. (23), and Antonino, et.al. (1).

FESEM: The surface morphology of the novel imine adsorbent for Cr ion before and after adsorption was cleared up by the FESEM (Field Emission Scanning Electron Microscope) to clarify the nature of the new imine. The imine surface is rough and, near-spherical in shape with an average diameter about 47 nm. The high porosity of its interval structure was observed as illustrated in Figure (2). Any slight change in the spherical surface morphology of adsorbent after adsorption process represented by an increase dramatically in the particle size to 74 nm due to adsorb of ion on the surface.

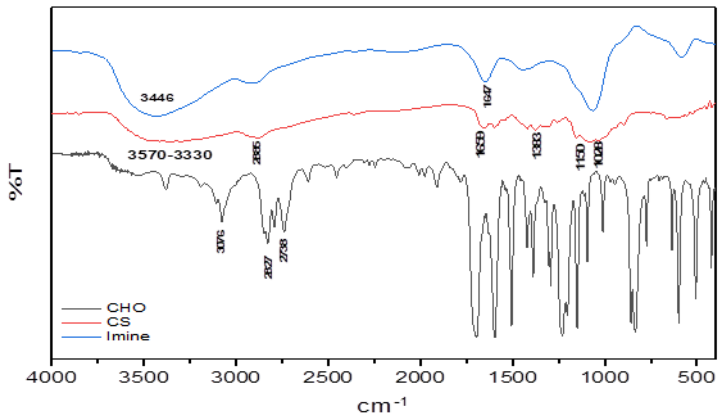

Figure 1. FTIR for chitosan,4-florobenzaldehyde and imine

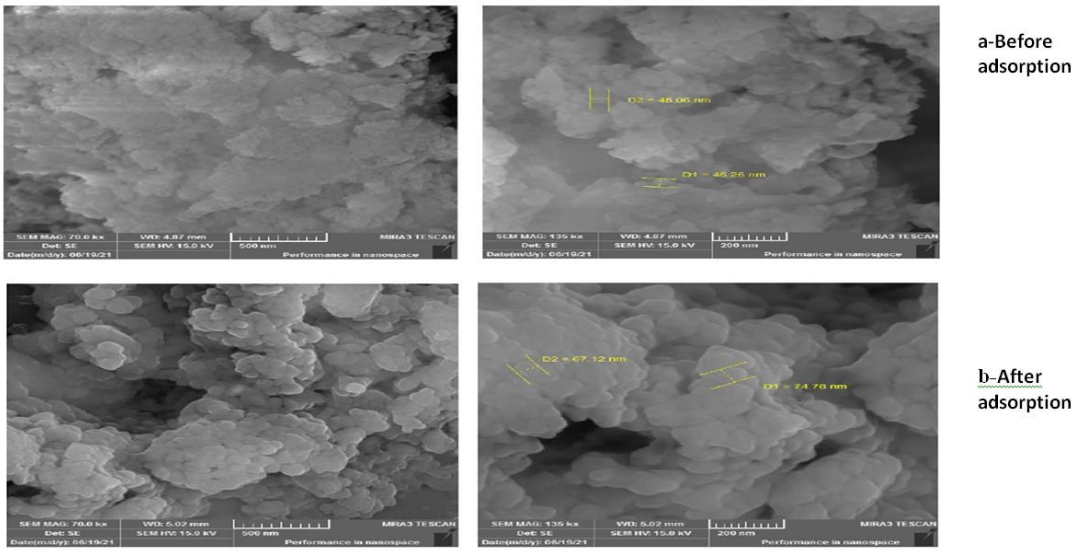

Figure 2. FESEM before and after adsorption of Cr (III) on imine

EDX: The element composition of imine, imine –Cr ion was determined by Energy Dispersive X-ray analysis, as flashed in Figure (3). Cr (III) is successfully put on the imine surface in Figure (3) on the left hand- side, but not on right side able to be seen. This indicates that the adsorption process has taken place sufficiently.

a-Before adsorption

b-After adsorption

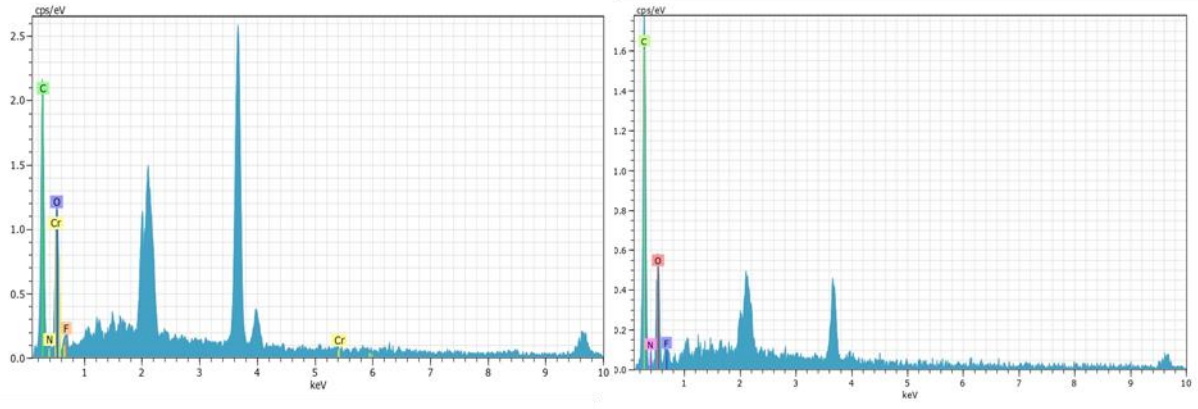

Figure 3. EDX for imine before and after adsorption of Cr (III) on imine

XRD: The crystallinity of the new adsorbent has changed, according to XRD analysis. The crystalline character of the carbon is shown by well-defined peaks, while the non-crystalline amorphous nature of the carbon is revealed by the hollow peak. In Figure (4), the XRD patterns of imine and imine with Cr (III) ions are presented. The XRD pattern of modified chitosan overload with Cr (III) ions is found to be somewhat different from that of unloaded modified biosorbent.= This indicates that Cr (III) ions may penetrate microspores and macrospores mainly through chemisorption, but also via physisorption, by changing the carbon structure (4, 12).

H-NMR: Figure (5), shows the H-NMR signal chemical shifts of the studied Schiff base – imine (3) (4-fluorobenzylidene)amino)-6 (hydroxymethyl)-2-methoxy-5-methyltetrahydro-2H-pyran-4-ol) recorded in DMSO .

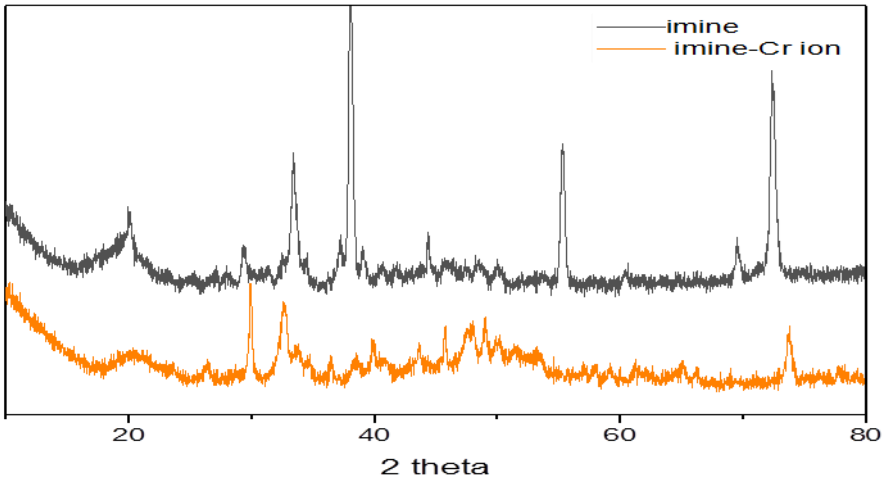

Figure 4. XRD pattern of imine biopolymer before and after adsorption

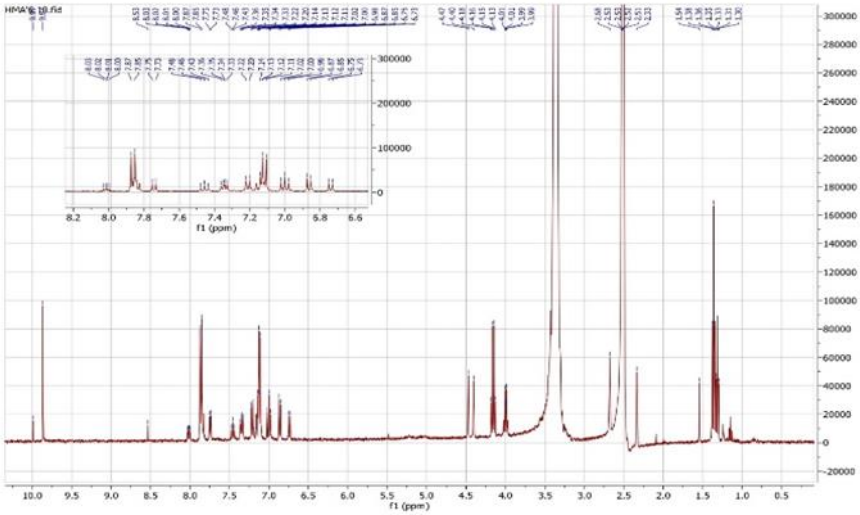

Figure 5. H-NMR for imine

The spectrum provides the following signals: phenyl as multiplet at 6.8-8 δ, -N-CH2 at (4.5δ), and C-CH=N- proton at 9.8ppm.This shifted occurrence in spectrum on account to high electronegativity of fluoride in aromatic ring (10, 24).

Adsorption time – kinetic study

The adsorbate possibly adsorbed onto a Schiff base adsorbent is essential for the form and management of an adsorption system, and exposure time is one of the functional variables in the procedures of batch adsorption. Figure (6), shows that the Cr (III) ion adsorption on imine process continued approximately 30 minutes at a high pace before gradually plateauing after 45 minutes of contact time. As is in view the diagram, the removal percentage increased rapidly in the first minutes, typically due to an enormous number of specific binding sites on the sorbent surface that were obtainable for the Cr ion. As time passed, the removal ratio gradually increased to 99 percent removal during 30 minutes and completely adsorbed for about 45 minutes. Furthermore, powerful

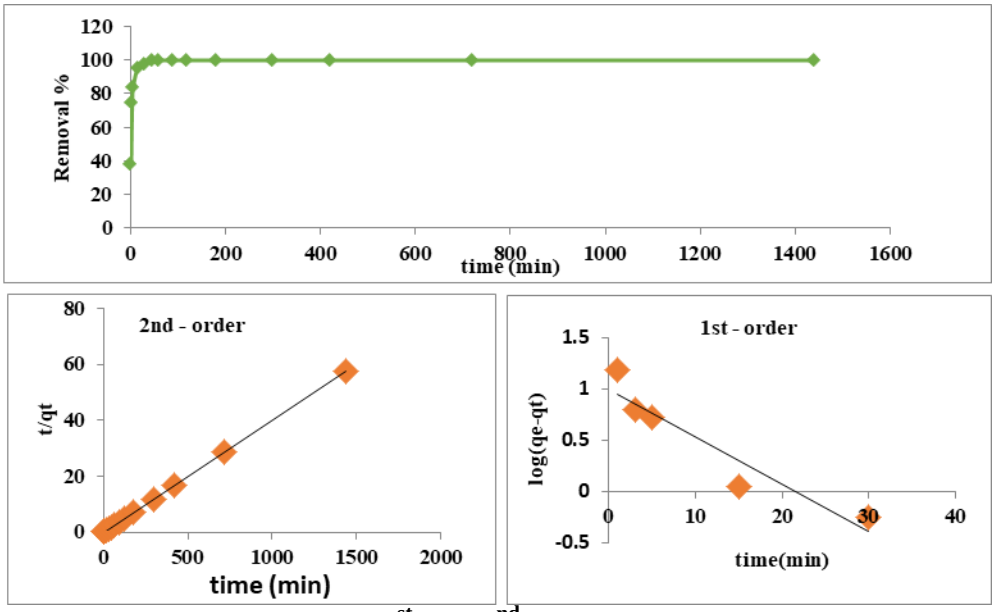

Figure 6. contact time, 1st and 2nd model of Cr (III) ion on imine

chelation and excellent affinity of imprinted sorbents were complimentary in size and form towards a template ion, resulting in a high uptake ratio of 100% in 45 minutes. Two kinetic models of the pseudo first order and pseudo second order were used to investigate the processes mechanism. The details of the calculation rate constant (k), adsorption capacity, and correlation coefficient (R^2) are shown in Table (1) below. Higher correlation coefficients of the pseudo second order model compared to the pseudo first order model are obvious. The consistency of the experiment results with the pseudo second order, as seen in Figure (6), indicates that Cr (III) ion adsorption process is governed by chemical adsorption, which involves valance forces via sharing or exchange of electrons between sorbent besides sorbate-imine

Table 1. Kinetic study parameters of Cr (III) removal onto imine

Adsorbents parameter	qe(mg/g)	Pseudo-first order kinetic parameter			Pseudo-second order kinetic		
R^2		q_{cal}(mg/g)	K(min^{-1})	R^2	q_{cal}(mg/g)	K (g/mg.min)	
Imine	25	9.93	0.10	0.8913	25	0.080	1

Effect of adsorption conditions

Effect of Ph: The impact of pH is investigated to identify the adsorption pH at which maximal metal removal occurs. Hydrochloric acid (HCl) or sodium hydroxide (NaOH) was used to adjust the pH from 3 to 11 at first (1.0 M and 0.1 M). Figure (7) shows the impact of pH on imine. The highest adsorption affinities for imine occur between pH 5 to 11. The speciation of adsorbate is pH-dependent; the active sites on an adsorbent may be protonated or deprotonated, which affects the adsorption of other ions. There is reduced metal ion absorption at lower pH values due to competing adsorption of H^+ and Cr (III) ions on the imine surfaces. The lower protonation reduces the number of metal ion binding sites. When the pH is increased, however, the absorption of Cr (III) increases. At the same time, the majority of active sites on the adsorbent is deprotonated, resulting in a stronger net attractive force, which accounts for the high chromium adsorption from solution. The optimal pH for adsorption is five. A rise in pH further hinders the adsorption process by precipitating chromium hydroxide complexes. As a consequence of the above findings, it was determined that chromium is strongly adsorbed in the imine, with a pH range of 99.9 %. At high pH values, adsorption decreases due to the formation of soluble hydroxyl complexes (7, 26).

Metal concentration affect

Impact of premier Cr (III) ion concentrations ranging from 30 ppm to 80ppm on removal percent was studied to assess the batch adsorption performance of Cr (III)-imine. As seen in Figure (8), raising the starting ion

concentration reduced the adsorption yields. As a result, when the initial concentration rises from 30ppm to 80ppm, the removal percent rises to about 100 percent. Still, when the concentration rises beyond 75 ppm, the percentage drops slightly and remains almost constant. This behaviour may be described in Cr (III) concentrations, resulting in the high removal efficiency. With higher starting Cr (III) concentrations and the same adsorbent mass, a scarcity of adsorption sites may develop, resulting in a decrease in removal effectiveness (19, 3).

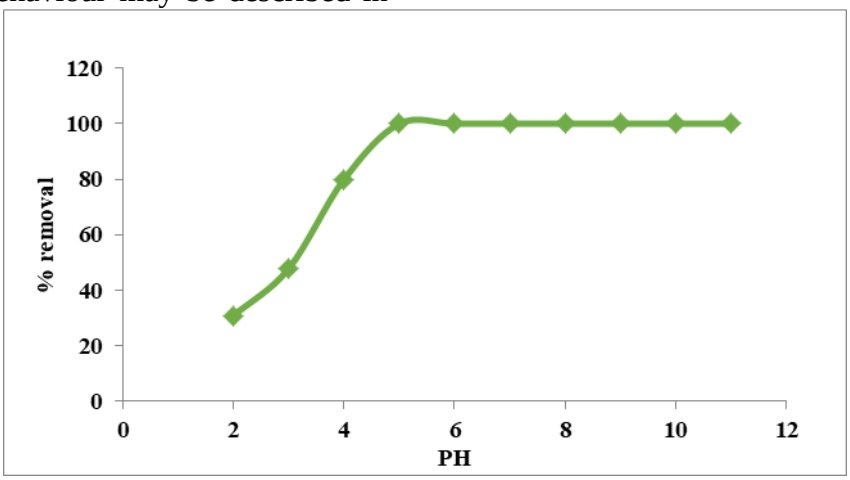

Figure 7. pH Effect Cr (III) ion on imine

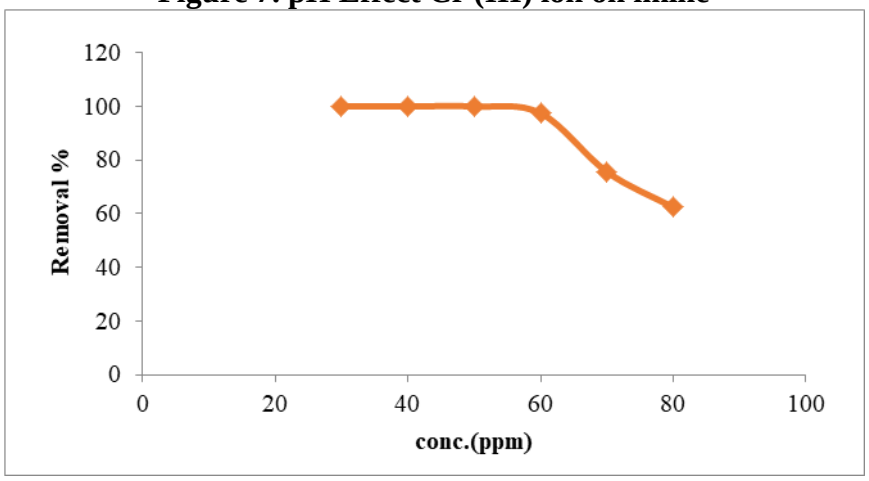

Figure 8. Effect of initial concentration of Cr (III) ion on imine

Dose effect of sorbet

On heavy metal ions sorption, the action of Schiff base weight was studied. The mass values ranged from 10-30 mg. Figure (9) depict the findings achieved. As can be observed, the optimal weight for imine was 20 mg, which resulted in 100% removal. Initially, the adsorption process increases quickly as the adsorbent mass increases, but after an optimal dose is achieved, it stays constant. This is most likely because the number of accessible active sites rose in proportion to the adsorbent dosage, resulting in an increase in removal efficiency. Any increase in the adsorbent concentration beyond this point had no discernible effect on the adsorption, which may be due to adsorption sites overlapping as a consequence of adsorbent particle overpopulation (19,7). Generally, 20 mg was taken as an optimum quantity for this work.

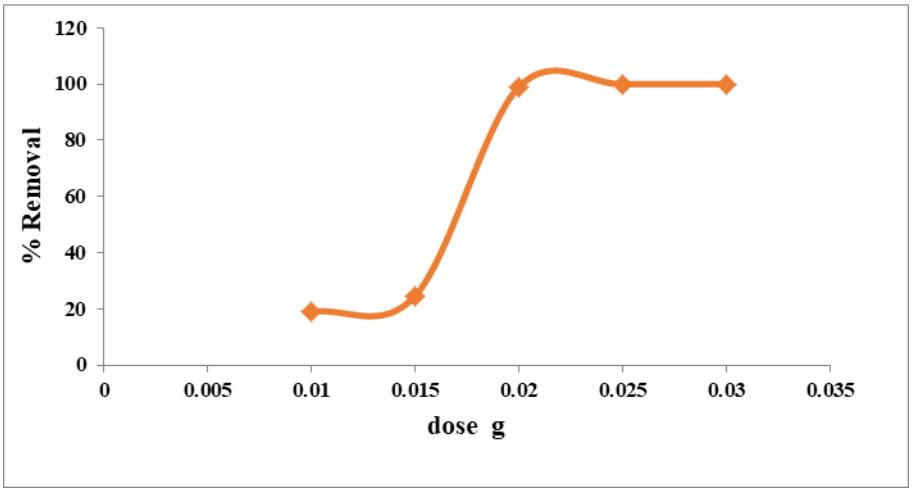

Figure 9. Aadsorbent dosage of Cr (III) ion on imine

Temperature effect- Thermodynamic study

The movement of molecules and ions in solution is influenced by temperature. This may be extended to ion adsorption since ions must be mobile to 'collide /interact' with the adsorbent and promote adsorption, particularly in adsorption process studies (14). Adsorption tests on various temperatures were done, and Cr (III) imine adsorption were measured; the results of those experiments are given in Figure (10), For imine adsorbent containing Cr ions, the adsorption study in a temperature range of 5-45C°. It is a key factor influencing adsorption of the sort in a system. Additionally, since most of adsorption processes are exothermic, lower temperatures promote adsorption removal. The figure illustrates that temperature has no impact on the imine's chromium adsorption capability. These findings indicate that chromium ions are adsorbed through an ionic process and that no coordinate kind of connection exists between the chromate ion and electron-rich donor atoms (18) As far thermodynamic factors governing Cr (III) adsorption on imine, according to thermodynamic principles, energy cannot be gained or lost in an isolated system. The only driving force is entropy change. To decide which process will be done spontaneously, both energy and entropy variables must be addressed in environmental engineering practice. K_d, the thermodynamic equilibrium constant, may be used to calculate the thermodynamic parameters. The following equations are used to compute the standard Gibbs free energy ΔG^o (kJ. mol^{-1}), standard enthalpy change ΔH^o (kJ. mol^{-1}), and standard entropy change ΔS^o ($J.mol^{-1}K^{-1}$), this information was taken from He, et.al. (9), and Fan, et.al. (5).

$$Kd = \frac{qe}{Ce} Kd = \frac{qe}{Ce}$$

$$\ln Kd = \frac{\Delta S}{R} + \frac{\Delta H}{RT} \ln Kd = \frac{\Delta S}{R} + \frac{\Delta H}{RT}$$

ΔG=-RT ln Kd

where R denotes the universal gas constant (8.314 J mol^{-1} K^{-1}); T denotes the absolute temperature (K); and K_d is the adsorption distribution constant deduced from qe/Ce (mg g^{-1}) The slope and intercept of the linear plot of ln Kd versus 1/T in Figure (10), were used to get the values of ΔH and ΔS, in contrast, the values of ΔG were determined using the equation above (9). Table (2) shows the negative $\Delta G°$ values imply that imine adsorption process is spontaneous. Energy change values drop somewhat as the temperature rises. This shows that, by raising the temperature, adsorption could be enhanced.

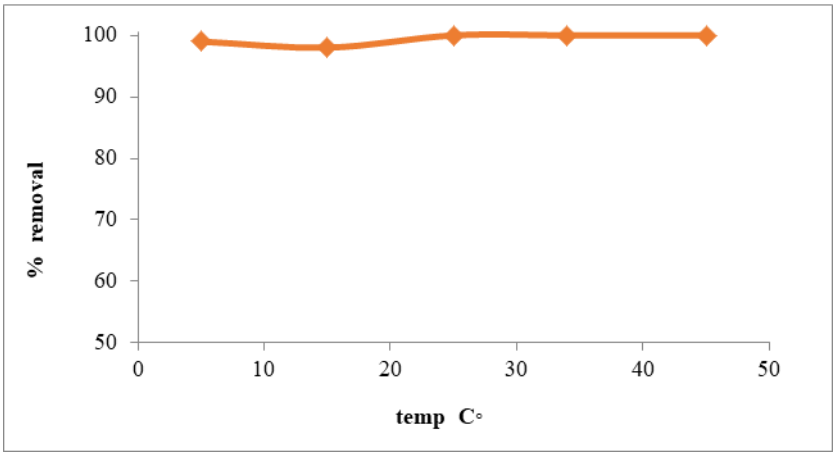

Figure 10. Temperature effect of Cr (III) ion on imine

Table 2. thermodynamic parameters of Cr (III) ions on to imine adsorption

	T(K)	ΔG(kJ/mole)	ΔH(kJ/mole)	ΔS(J/mol.K)
Imine	278	-9.01	+108.69	+419.41
	288	-7.63		
	298	-21.05		
	308	-21.78		
	318	-22.47		

Positive entropy and enthalpy values also show the endothermic nature of Cr (III) adsorption on imine. Increases in the temperature of the solution have no impact on the adsorption (18). Chemisorption is prevalent in the findings. The positivity. The positivity of ΔS indicates a strong unpredictability at the solid/solution interfaces. When ΔG goes to 0 (negative value), Cr (III) adsorption on biosorbent is spontaneously taking place.

Isotherms models study

The adsorption isotherm behavior of Cr (III) by produced materials was investigated using three different kinds adsorption isotherm models. The methods of Langmuir, Freundlich, and Temkin were used. Figure (11), shows the linear regression of the Cr (III) adsorption isotherm models onto Schiff base (Table 3) shows the factors and coefficients of correlation for Langmuir, Freundlich, and Temkin. The Langmuir isotherm had the greatest correlation coefficient (R^2) in the case of imine, suggesting that the adsorption mechanism was monolayer adsorption. High adsorption ability can be explained by higher values of K_L and R^2 for Cr (III) - imine which are 5.12 L/mg, 0.9992, respectively, indicating that the solute and adsorbent have a higher affinity. Another reason could be that the active sites are relatively evenly dealt on the surface and inside the adsorbent (22,28,9). In this study R_L value with range (0.006-0.0027). were all within 0 and 1, indicating an extremely favorable adsorption with increasing adsorption efficiency at higher Cr (III) concentrations (13).

Table 3. Isotherm models correlation coefficients and constant for adsorption of Cr (III) on imine

		Langmuir		Freundlich		Temkin
Imine (Schiff base)	q_m	26.8 mg/g	1/n	0.0811	at	26.148
	K_l	5.12	Kf	25.28	bt	1.858
	R^2	0.9992	R^2	0.6457	R^2	0.7043
	R_L	(0.006-0.0027)				

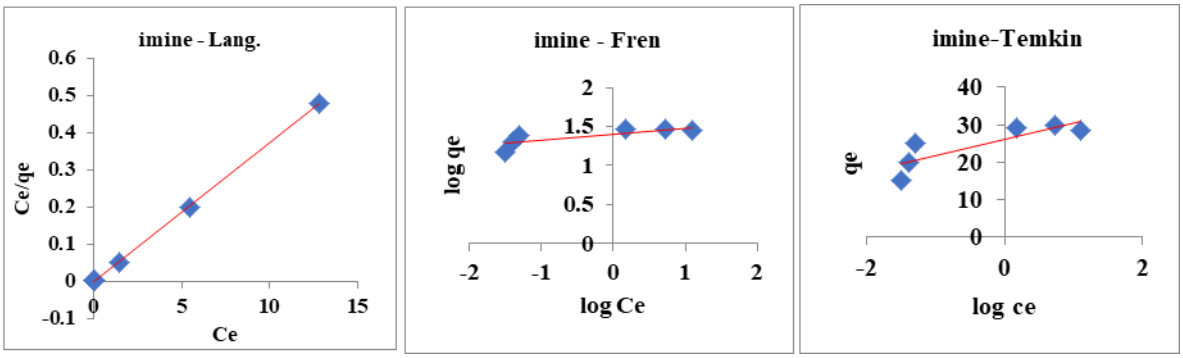

Figure 11. Adsorption Cr (III), Langmuir, Freundlich and Temkin isotherm model

Desorption and reuse

The capacity to be readsorbed and reused is one of the most important characteristics that make an adsorbent useful and essential for improving process economics. The Schiff base adsorbents, which have Cr (III) adsorbed on their surface, will be next dehydrated and treated with 0.1 M EDTA and 0.1M HCl solutions. The adsorption/desorption tests are then repeated five times for Schiff base adsorption-desorption periods (Figure 12).

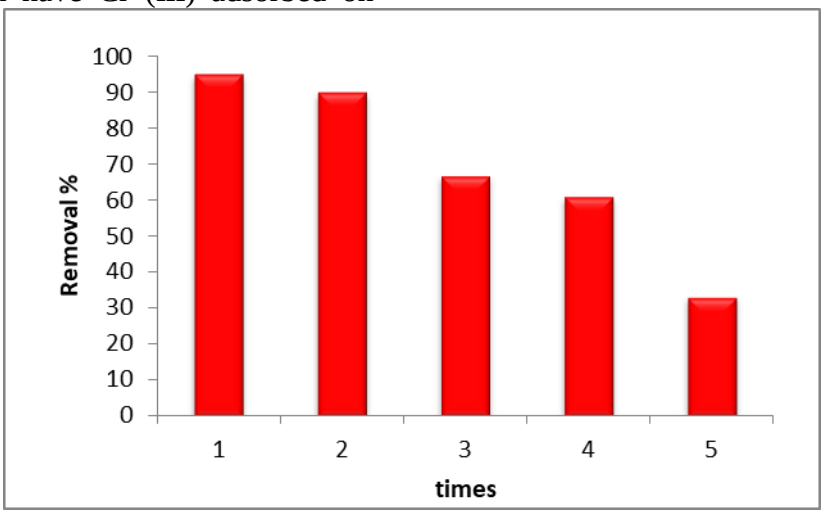

Figure 12. Reusability of imine for removal percent to Cr (III

Table 4. Determination of Cr (III) ion in tow supplement

Samples	Amount added µg/mL	Amount found µg/mL	RSD	Recovery %
H.M supplument	0	5	± 1.2	-
	30	34.91	± 0.4	99.74
	50	54.74	± 0.8	99.52
M.V Supplument	0	0	0	-
	30	29.78	± 0.92	99.26
	50	49.23	± 1.32	98.46

Application of real sample

To obtain controls for the study, as shown in Table 4, samples were spiked with Cr (III) ions to supplement tablets. After the batch experiment, the recovery of Cr (III) ions in real and spiked samples varied in range (98.4-99.92) %, and relative standard deviation was less than (3.1) The results support the sensitivity and reliability of adsorbent toward spike and non-spike for preconcentration and determination of these ion in trace value.

CONCLUSION

Functionalized chitosan–Schiff base has been successfully achieved from the free amino group of chitosan and aldehyde to remove Cr (III) from solution. Langmuir and pseudo 2nd order model were more fitted data with good correlation coefficients. The removal ratio of heavy metal reached 100% for Cr(III) 50ppm, 20mg adsorbent dose for 30min using normal adsorbent pH at different Temperatures. Imine was not only high in removal efficiency but also had simple preparation and good

reusability; it showed high response for trace amount of chromium ion in real sample.

REFERENCES

1. Antonino, R., B. Fook, V. Lima, R. D. F. Rached, E. Lima, R. S. Lima, C. P. Covas and M. L. Fook, 2017. Preparation and characterization of chitosan obtained from shells of shrimp (*Litopenaeus vannamei Boone*). Mar. Drugs, 15**,** 1-12. Doi.org/10.3390/md15050141.

2. Ayawei, N., 2017. Augustus Newton Ebelegi, and Donbebe Wankasi. Modelling and interpretation of adsorption isotherms. Hindawi Journal of Chemistry. Doi.org/10.1155/2017/3039817.

3. Dao, M. U., H. S. Le, V. D. Doan, and H. T. Nguyen, 2019. Adsorption of Ni (II) ions by magnetic activated carbon/chitosan beads prepared from spent coffee grounds, shrimp shells and green tea extract. Environmental Technology.40,1-49. Doi.org/10.1080/09593330.2019.1584250

4. Elavarasan, A. 2018. EDX and XRD, FT-IR spectra, analysis containing hexavalent chromium metal ion adsorption present in aqueous solution on to phosphoric acid (H_3PO_4) activated Mimusops elengi leaves carbon. Journal of Drug Delivery and Therapeutics, 8**,** 132-138. Doi.org/10.22270/jddt.v8i5-s.1917.

5. Fan, H. T., X. T. Sun, Z. G. Zhang, and W. X. LI, 2014. Selective removal of lead (II) from aqueous solution by an ion-imprinted silica sorbent functionalized with chelating N-donor atoms. Journal of Chemical and Engineering Data, 59**,** 2106-2114. Doi.org/10.1021/je500328t.

6. Gatabi, J., Y. Sarrafi, M. M. Lakouraj, and M. Taghavi, 2020. Facile and efficient removal of Pb (II) from aqueous solution by chitosan-lead ion imprinted polymer network. Chemosphere, 240**,** 124772. Doi.org/10.1016/j.chemosphere.2019.124772.

7. Gokila, S., T. Gomathi, P. Sudha, and S. Anil, 2017. Removal of the heavy metal ion chromiuim (VI) using Chitosan and Alginate nanocomposites. International Journal of Biological Macromolecules, 104**,** 1459-1468. Doi.org/10.1016/j.ijbiomac.2017.05.117.

8. Hassan, R., H. Arida, M. Montasser, and N. Abdel Latif, 2013. Synthesis of new Schiff base from natural products for remediation of water pollution with heavy metals in industrial areas. Journal of Chemistry, 2013. Doi.org/10.1155/2013/240568.

9. He, Y., P. Wu, W. Xiao, G. Li, J. Yi, Y. He, C. Chen, P. Ding and Y. Duan, 2019. Efficient removal of Pb (II) from aqueous solution by a novel ion imprinted magnetic biosorbent: adsorption kinetics and mechanisms. PLoS One, 14**,** e0213377. Doi.org/10.1371/journal.pone.0213377.

10. Issa, Y., H. Hassib and H. Abdelaal, 2009. 1H NMR, 13C NMR and mass spectral studies of some Schiff bases derived from 3-amino-1, 2, 4-triazole. Spectrochimica Acta Part A: Molecular and Biomolecular Spectroscopy, 74**,** 902-910. Doi.org/10.1016/j.saa.2009.08.042.

11. Kocak, N., M. Sahin, G. Arslan, and H. I. Ucan, 2012. Synthesis of crosslinked chitosan possessing schiff base and its use in metal removal. Journal of Inorganic and Organometallic Polymers and Materials, 22**,** 166-177. Doi.org/10.1007/s10904-011-9509-3.

12. Kofa, G., G. Nkoue Ndongo, K. Ngounou, M. Nsoe, E. Amba and S. Ndi Koungou, 2019. Grewia spp. Biopolymer as Low-Cost Biosorbent for Hexavalent Chromium Removal. Journal of Chemistry, 2019. Doi.org/10.1155/2019/6505731.

13. Li, H., J. Li, and L. Cheng, 2015. Novel Cr (III) surface magnetic ion-imprinted materials based on graphene oxide for selective removal of Cr (III) in aqueous solution. Desalination and Water Treatment, 56**,** 204-215. Doi.org/10.1080/19443994.2015.1025852.

14. Mafu, L. D., B. B. Mamba, and T. A. Msagati, 2016. Synthesis and characterization of ion imprinted polymeric adsorbents for the selective recognition and removal of arsenic and selenium in wastewater samples. Journal of Saudi Chemical Society, 20**,** 594-605. Doi.org/10.1016/j.jscs.2014.12.008.

15. Monier, M., A. A. H. Bukhari, and N. H. Elsayed, 2020. Designing and characterization of copper (II) ion-imprinted adsorbent based on isatin functionalized chitosan. International Journal of Biological Macromolecules, 155**,** 795-804. Doi.org/10.1016/j.ijbiomac.2020.03.215

16. Mustafa H.N and I. Al -Ogaidi, 2023. Efficacy of zinc sulfide- chitosan nanoparticles against bacterial diabetic wound infection. Iraqi Journal of Agricultural Sciences.54(1):1-17. https://doi.org/10.36103/ijas.v54i1.1671

17. Nisreen A. J. and M. M. Sirhan,2021. Comparative study of removal pollutants (heavy metals) by agricultural wastes and other chemical from the aqueous solutions. Iraqi Journal of Agricultural Sciences. 52(2):392-402. https://doi.org/10.36103/ijas.v52i2.1300

18. Neagu, V. 2009. Removal of Cr (VI) onto functionalized pyridine copolymer with amide groups. Journal of Hazardous Materials, 171**,** 410-416. Doi.org/10.1016/j.jhazmat.2009.06.016.

19. Nematidil, N., M. Sadeghi, S. Nezami, and H. Sadeghi, 2019. Synthesis and characterization of Schiff-base based chitosan-g-glutaraldehyde/NaMMTNPs-APTES for removal Pb^{2+} and Hg^{2+} ions. Carbohydrate Polymers, 222**,** 114971. Doi.org/10.1016/j.carbpol.2019.114971.

20. Puvvada, Y. S., S. Vankayalapati, and S. Sukhavasi, 2012. Extraction of chitin from chitosan from exoskeleton of shrimp for application in the pharmaceutical industry. International Current Pharmaceutical Journal, 1**,** 258-263.

21. Raghad N. M and I. A. Abeer. 2023. Adsorption of methylene blue from aqueous solution using free and immobilized algae cells. Iraqi Journal of Agricultural Sciences. 54(5),1387-1397. https://doi.org/10.36103/ijas.v54i5.1839

22. Ren, Y., M. Zhang, and D. Zhao, 2008. Synthesis and properties of magnetic Cu (II) ion imprinted composite adsorbent for selective removal of copper. Desalination, 228**,** 135-149. Doi.org/10.1016/j.desal.2007.08.013

23. Shahraki, S., H. S. Delarami, F. Khosravi, and R. Nejat, 2020. Improving the adsorption potential of chitosan for heavy metal ions using aromatic ring-rich derivatives. Journal of Colloid and Interface Science, 576**,** 79-89. Doi.org/10.3390/md15050141.

24. Thatte, C., M. Rathnam, and A. Pise, 2014. Chitosan-based Schiff base-metal complexes (Mn, Cu, Co) as heterogeneous, new catalysts for the β-isophorone oxidation. Journal of Chemical Sciences, 126**,** 727-737. Doi.org/10.1007/s12039-014-0601-4.

25. Vadivel, T., M. S. Dhamodaran, Kulathooran, and S. Senguttuvan, 2020. Rhodium (III) complexes derived from complexation of metal with azomethine linkage of chitosan biopolymer Schiff base ligand: Spectral, thermal, morphological and electrochemical studies. Carbohydrate Research,487**,**107878. Doi.org/10.1016/j.carres.2019.107878.

26. Wahab, M. A., S. Jellali, and N. Jedidi, 2010. Effect of temperature and pH on the biosorption of ammonium onto Posidonia oceanica fibers: Equilibrium, and kinetic modeling studies. Bioresource Technology, 101**,**8606-8615. Doi.org/10.1016/j.biortech.2010.06.099.

27. Yunus, K., M. Zuraidah, and A. John, 2020. A review on the accumulation of heavy metals in coastal sediment of Peninsular Malaysia. Ecofeminism and Climate Change.1,1-35. Doi.org/10.1108/EFCC-03-2020-0003.

28. Zhang, Y., Z. Bai, W. Luo, L. Zhai, B. Wang, X. Kang, and J. Zong, 2019. Ion imprinted adsorbent for the removal of Ni (II) from waste water: preparation, characterization, and adsorption. Journal of Dispersion Science and Technology, 40**,** 1751-1760. Doi.org/10.1080/01932691.2018.1538883.

29. Zhou, Z., D. Kong and Z. Ren, 2018. Preparation and adsorption characteristics of an ion-imprinted polymer for fast removal of Ni (II) ions from aqueous solution. Journal of Hazardous Materials, 341**,** 355-364. Doi.org/10.1016/j.jhazmat.2017.06.010.